

**PEAK CLADDING TEMPERATURE
IN A SPENT FUEL STORAGE OR TRANSPORTATION CASK**

Jie Li,¹ Haruko Murakami,¹ Yung Liu,¹ P.E.A. Gomez,² Mithum Gudipati,² and Miles Greiner²

¹Argonne National Laboratory ²University of Nevada
Argonne, IL 60439 Reno, NV 89557

ABSTRACT

From reactor discharge to eventual disposition, spent nuclear fuel assemblies from a commercial light water reactor are typically exposed to a variety of environments under which the peak cladding temperature (PCT) is an important parameter that can affect the characteristics and behavior of the cladding and, thus, the functions of the spent fuel during storage, transportation, and disposal. Three models have been identified to calculate the peak cladding temperature of spent fuel assemblies in a storage or transportation cask: a coupled effective thermal conductivity and edge conductance model developed by Manteufel and Todreas, an effective thermal conductivity model developed by Bahney and Lotz, and a computational fluid dynamics model. These models were used to estimate the PCT for spent fuel assemblies for light water reactors under helium, nitrogen, and vacuum environments with varying decay heat loads and temperature boundary conditions. The results show that the vacuum environment is more challenging than the other gas environments in that the PCT limit is exceeded at a lower boundary temperature for a given decay heat load of the spent fuel assembly. This paper will highlight the PCT calculations, including a comparison of the PCTs obtained by different models.

INTRODUCTION

A spent fuel storage and/or transportation cask typically contains 24 assemblies for pressurized water reactors (PWRs) or 68 assemblies for boiling water reactors (BWRs). Individual fuel pins number $\approx 6,300$ for a PWR cask and $\approx 4,300$ for a BWR cask. The spent fuel assemblies are placed within a grid-like basket inside a canister or cask, and the loading of the spent fuel assemblies is conducted under water in the spent fuel pool. The canister or cask must be drained, rendered dry, and backfilled with a cover gas (e.g., helium) before welding (canister) or bolted closure (cask) for subsequent dry storage and/or transportation. After the transportation cask is delivered to its destination, i.e., the Yucca Mountain repository or other centralized locations for (interim) storage or reprocessing, the spent fuel assemblies may be stored or retrieved from the cask at the surface facility of these locations. In the latter instance, the spent fuel may be exposed to air and oxidize if the cladding is damaged during handling and transportation. The resulting volume expansion of the fuel could “unzip” the cladding, thus greatly increasing the potential for release of radioactivity and contamination.

Heat transfer in a spent fuel storage and/or transportation cask has been studied in the past to determine the factors that would affect the PCT of the spent fuel. The studies often involved analytical, numerical, and experimental investigations of conduction, radiation, and natural convection of decay heat in the spent nuclear fuel (SNF) assemblies in a cask situated either vertically or horizontally, which are the typical orientations of casks in dry storage and transportation, respectively. (Exceptions are the NUHOMS dry cask systems that store the SNF assemblies horizontally.) A potential concern for high-

burnup (≥ 45 GWd/MTU) cladding is related to the formation of radial hydrides in the cladding after the spent fuel is removed from the spent fuel pool for dry storage or transportation.³ Depending on the decay heat of the spent fuel and the drying operation, an unfavorable radial hydride distribution may develop in the cladding, rendering it prone to failure, especially during a drop accident. The factors involved in radial hydride formation are the hydrogen content, temperature, hoop stress in the cladding, and the duration of drying, including the rate of cooling.⁴ The peak cladding temperature and hoop stress during drying depend on the decay heat load of the SNF assemblies, the heat transfer characteristics (conduction, convection, and radiation), and the environment of the loaded cask, as does the cooling rate of the SNF assemblies from the peak cladding temperature.

MODELING OF PEAK CLADDING TEMPERATURE

Three heat transfer models were employed in the calculation of PCTs of SNF assemblies (PWR and BWR) in a storage or transportation cask: (1) A two-region model that emphasizes conduction and radiation;¹ (2) an effective thermal conductivity (ETC) model developed based on the finite element analysis of solids;² and (3) a computational fluid dynamics (CFD) model that emphasizes conduction and natural convection. The PCTs are calculated as a function of decay heat of the SNF assemblies, the assembly wall temperature, and the interior environment of the cask, i.e., vacuum, helium, or nitrogen (taken as air) that represents, respectively, the most challenging periods of drying, storage and transportation, and receiving at the surface facility of the Yucca Mountain repository or other centralized locations for storage or reprocessing.

Two-Region Model

Figure 1 shows the two-region model developed by Manteufel and Todreas.¹ The SNF assembly is represented by two regions - an interior region characterized by an effective thermal conductivity (k_{eff}), and an edge region characterized by a thermal conductance (h_{edge}). Two modes of heat transfer are considered in the interior region of the assembly: stagnant-gas conduction and thermal radiation. The combined conductive and radiative conductivities (i.e., k_{cond} and k_{rad}) yield

$$k_{eff} = k_{cond} + k_{rad} \quad (1)$$

with

$$k_{cond} = F_{cond} k_{gas} \quad \text{and} \quad k_{rad} = C_{rad} \sigma \pi d T^4 \quad (2)$$

where F_{cond} is a conduction factor that depends on the volume fraction of the fuel pins, pin geometry, the thermal conductivity of the cladding, and the thermal conductivity of the backfill gas (k_{gas}); C_{rad} is a radiative coefficient that depends on the fuel-pin emissivity and a pin-to-pin absorption factor; σ is the Stefan-Boltzmann constant; d is the pin diameter; and T is the temperature. Representative values of F_{cond} are 2.1 for helium and 2.4 for nitrogen, and a representative value of C_{rad} is 0.4, according to Manteufel and Todreas.¹

Similar to the interior model, the edge model also considers stagnant-gas conduction and radiation, i.e.,

$$h_{edge} = h_{cond} + h_{rad} \quad (3)$$

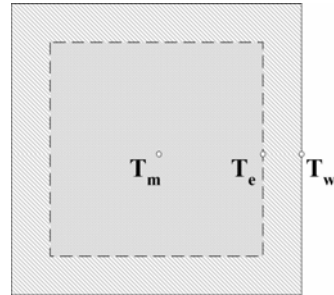


Fig. 1 Locations of the maximum, extrapolated, and wall temperatures in a two-region, k_{eff}/h_{edge} model

where h_{cond} and h_{rad} possess functional forms similar to those of Eq. (2) after having been divided by a characteristic length, i.e., $h = k/(\text{characteristic length})$. The conduction factors and the radiative coefficient in the edge model depend also on the thermal properties of the enclosure wall, in addition to the thermal properties of the pin cladding and the backfill gas. The resulting lumped $k_{\text{eff}}/h_{\text{edge}}$ model is represented by two coupled, nonlinear algebraic equations:

$$Q = C_1(T_m - T_e) + C_2(T_m^4 - T_e^4) \quad (4)$$

$$Q = C_3(T_e - T_w) + C_4(T_e^4 - T_w^4) \quad (5)$$

for the interior region and the edge region of the assembly, respectively. In these equations, Q is the total assembly decay power; and T_m , T_e , and T_w are the maximum, extrapolated, and wall temperatures depicted in Fig. 1, respectively. The locations of T_m and T_w are self-evident; T_e is located at an imaginary surface corresponding to the extrapolated boundary of the interior region. The nonlinear heat conduction equation for the interior region of the assembly is solved by assuming that heat generation is spatially uniform, and the extrapolated wall temperature is circumferentially uniform. The temperature dependence of the radiative component of k_{eff} is solved by Kirchoff's transformation. Using values for the parameters of typical BWR (8 x 8) and PWR (15 x 15) spent fuel assemblies, Manteufel and Todreas¹ obtained the coefficients in the lumped $k_{\text{eff}}/h_{\text{edge}}$ model in Eqs. (4) and (5), which are listed in Table 1.

Table 1 Coefficients in the lumped $k_{\text{eff}}/h_{\text{edge}}$ model for a typical BWR (8 x 8) and PWR (15 x 15) spent-fuel assembly in helium, nitrogen, and vacuum environment*

	C_1 (W/K)	C_2 (10^{-8} x W/K ⁴)	C_3 (W/K)	C_4 (10^{-8} x W/K ⁴)
BWR, He	17.38	3.6	36.54	2.49
BWR, N ₂	3.97	3.6	7.07	2.31
BWR, vacuum	0	3.6	0	2.31
PWR, He	17.38	3.16	64.0	3.83
PWR, N ₂	3.97	3.16	12.38	3.55
PWR, vacuum	0	3.16	0	3.55

*Coefficient values for He and N₂ environment are those of Manteufel and Todreas¹; those for vacuum are deduced by ignoring the stagnant-gas conduction, i.e., $C_1 = C_3 = 0$.

A nonlinear equation solver, *Mathematica*, was used to solve Eqs. (4) and (5) as a function of the total assembly decay power Q and the average enclosure wall temperature T_w . The resulting T_m and T_e will be shown later.

Effective Thermal Conductivity (ETC) Model

The effective thermal conductivity (ETC) model was developed by Bahney and Lotz² based on finite element (ANSYS) thermal analyses of various SNF assemblies with fill gas environments of helium, vacuum, nitrogen, and argon. The three major heat transfer processes, i.e., conduction, radiation, and convection, in a spent fuel assembly are represented by a smeared, or homogenized, effective thermal conductivity. The ETC model is similar to the lumped $k_{\text{eff}}/h_{\text{edge}}$ model; the difference between them is that the radiative and conductive components in Eqs. (2) and (3) are embedded in the nonlinear temperature-dependent terms in the ETC correlations shown in Tables 2 and 3, respectively, for a PWR and BWR SNF assembly, each under a different set of environments.

Table 2 Effective thermal conductivity (ETC) correlations for PWR fuel assembly²

Fuel assembly	Gas	ETC (W/m°C)	
PWR (14 x 14)	He	$0.3490 + 1.334 \times 10^{-3}T_m + 2.849 \times 10^{-6}T_m^2 + 8.359 \times 10^{-10}T_m^3$	(6a)
PWR (17 x 17)	vacuum	$0.0678 + 6.483 \times 10^{-4}T_m + 2.825 \times 10^{-6}T_m^2 + 1.644 \times 10^{-9}T_m^3$	(6b)
	N ₂	$0.1219 + 8.182 \times 10^{-4}T_m + 2.698 \times 10^{-6}T_m^2 + 1.514 \times 10^{-9}T_m^3$	(6c)
	Ar	$0.1055 + 7.953 \times 10^{-4}T_m + 2.513 \times 10^{-6}T_m^2 + 1.916 \times 10^{-9}T_m^3$	(6d)

Table 3 Effective thermal conductivity (ETC) correlations for BWR fuel assembly²

Fuel assembly	Gas	ETC (W/m°C)	
BWR (9 x 9)	He	$0.2668 + 8.750 \times 10^{-4}T_m + 2.513 \times 10^{-6}T_m^2$	(7a)
	vacuum	$0.0562 + 3.630 \times 10^{-4}T_m + 2.801 \times 10^{-6}T_m^2 + 3.640 \times 10^{-10}T_m^3$	(7b)
	N ₂	$0.0913 + 4.680 \times 10^{-4}T_m + 2.861 \times 10^{-6}T_m^2$	(7c)
	Ar	$0.0820 + 4.090 \times 10^{-4}T_m + 2.997 \times 10^{-6}T_m^2 + 1.627 \times 10^{-10}T_m^3$	(7d)

The temperature T_m in Eqs. (6) and (7) is the mean temperature of the assembly, i.e.,

$$T_m = (T_{cen} + T_{surf})/2 \quad (8)$$

where T_{cen} and T_{surf} are, respectively, the center temperature (PCT) and the surface (basket) temperature of the assembly. The temperature drop, $\Delta T = T_{cen} - T_{surf}$, for a smeared, homogeneous heat-generating square is given by

$$\Delta T = 0.2947 Q / [4L(ETC)] \quad (9)$$

where Q is the assembly decay heat load (W), L is the active assembly length (m), and ETC (W/m°C) is given by Eqs. (6) and (7).

Computational Fluid Dynamics (CFD) Model

The CFD models are constructed for a BWR (7 x 7) SNF assembly and for twenty-one (21) PWR (15 x 15) SNF assemblies in a canister, shown in Fig. 2(a) and 2(b), respectively. The FLUENT code was used to calculate the PCTs. Conduction and radiation temperature results were determined by solving the steady-state energy equation using a finite volume method with a second-order discretization scheme. For natural convection/radiation simulations, the steady-state conservation of momentum equations were solved with a second-order upwind scheme to obtain velocity and pressure fields. All of the cases were run for conduction/radiation and for radiation/natural convection to quantify the effects of natural convection on the BWR (7 x 7) spent fuel assembly with helium and nitrogen backfill.

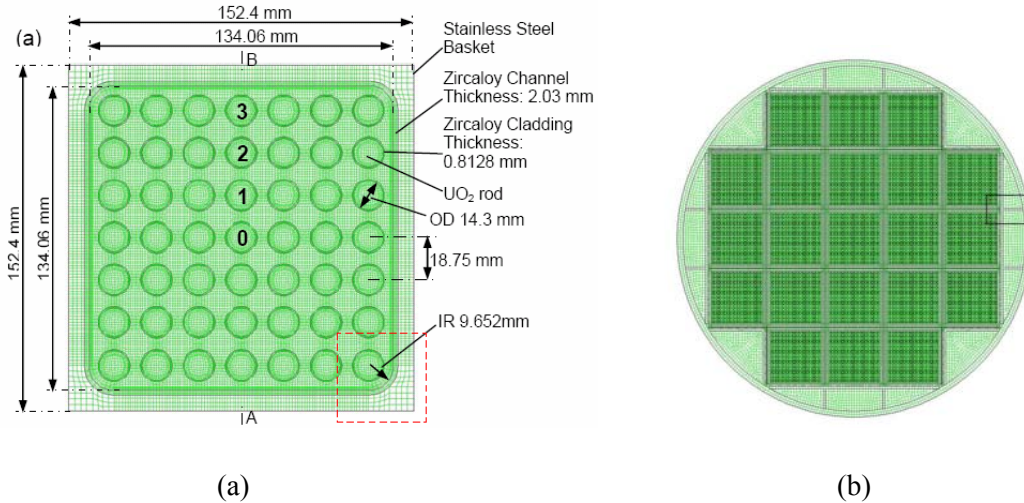


Figure 2. Computational grid for PCT calculations: (a) a BWR (7 x 7) SNF assembly, and (b) 21 PWR (15 x 15) SNF assemblies in a canister.

Figure 2(a) shows the detailed grid information for a BWR (7 x 7) fuel assembly. Calculations were performed with uniform wall temperatures of $T_w = 25^\circ\text{C}$ and 400°C , and fuel assembly heat generation rates of $Q = 100, 200, 300, 400, 500,$ and 600 W. The volumetric heat generation rate within the fuel pellets was determined from dividing the assembly Q by the total volume of the fuel pellets in the assembly. A peaking factor of 1.25 was applied to account for the higher heat generation at the axial center of the assembly. The details for handling voids can be found in an early paper.⁵ The BWR model was initially run with only conduction and radiation, with helium and nitrogen backfill.

The dot-filled regions in Fig. 2(b) represent twenty-one (21) PWR (15 x 15) spent fuel assemblies in a canister, originally modeled after the multi-purpose canister.⁶ By coincidence, this is very similar to the geometry and loading configuration of the Transport, Aging and Disposal (TAD) canister system that the Department of Energy Office of Civilian Radioactive Waste Management plans to use for the bulk of the commercial PWR spent fuel assemblies destined for the Yucca Mountain repository.⁷

RESULTS AND DISCUSSION

Two-region Model: Figures 3 and 4 show the PCTs calculated by the two-region model for a PWR (15 x 15) spent fuel assembly over a range of assembly wall temperatures ($T_w = 25$ to 350°C) and decay heat loads ($Q = 100$ to $2,000$ W) in various gaseous environments. The PCTs were determined from solving the coupled nonlinear Eqs. (4) and (5), with the appropriate coefficients C_1 to C_4 from Table 1.

The calculated PCTs in the vacuum environment are significantly higher than the PCTs calculated in the nitrogen or helium environment. For a given wall temperature T_w , the PCT increases with the decay heat load most dramatically in vacuum, as indicated by a larger slope of the red

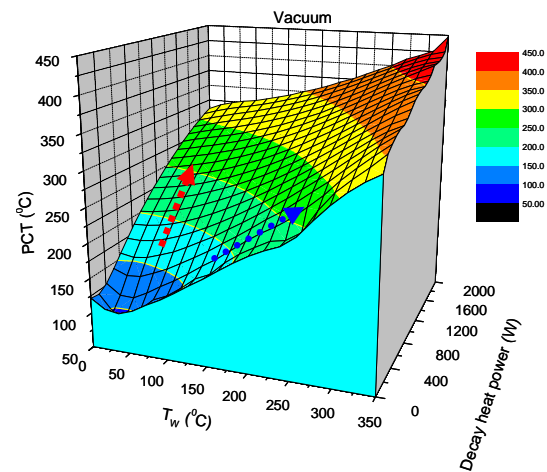


Fig. 3. Calculated PCTs for a PWR (15 x 15) spent fuel assembly in vacuum.

arrow in Fig. 3, versus those in Fig. 4 (a) and (b). For a given decay heat load Q , ΔT decreases with increasing T_w in all three fill-gas environments; for example, ΔT values are 136, 86, and 55°C for $T_w = 100, 200,$ and 300°C , respectively, with $Q = 800$ W in vacuum (see Fig. 3).

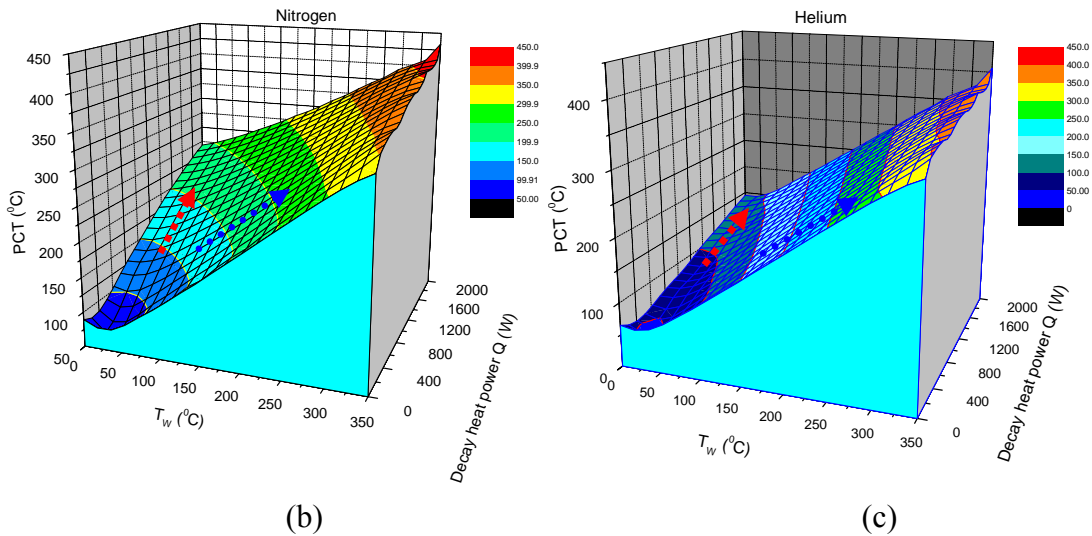


Fig. 4. Calculated PCTs for a PWR (15 x 15) spent fuel assembly in nitrogen, (b), and helium, (c), over a range of assembly wall temperatures (T_w) and decay heat loads (Q)

If one takes 350°C as the limit for the PCT, Figs. 3 and 4 show the orange-colored demarcation boundaries above which the combination of T_w and Q that would give $\text{PCT} \geq 350^\circ\text{C}$. As an example, the calculated PCT is 351°C for $Q = 2,000$ W and $T_w = 150^\circ\text{C}$ in a vacuum.

Effective Thermal Conductivity (ETC) Model: Table 4 shows the PCTs calculated from the ETC correlations for a BWR (9 x 9) spent fuel assembly in the various environments, based on Eqs. (7), (8) and (9). Again, the highest PCTs are obtained for the vacuum environment, and the lowest PCTs are obtained for the helium environment. The differences in the PCTs are slight, however, among vacuum, nitrogen and argon.

Table 4 Calculated PCTs for a BWR spent fuel assembly

BWR (9 x 9)		Helium					
$T_w(^{\circ}\text{C})/Q(\text{W})$	100	200	400	800	1000	1500	2000
25	28	32	38	50	56	69	82
50	53	56	62	73	79	91	103
100	103	105	110	120	124	135	145
150	152	154	159	167	171	180	189
200	202	204	207	214	217	226	233
250	252	253	256	262	265	272	279
300	301	303	305	310	313	319	325
350	351	352	355	359	361	366	371

BWR (9 x 9)		Vacuum					
$T_w(^{\circ}\text{C})/Q(\text{W})$	100	200	400	800	1000	1500	2000
25	39	50	68	95	105	127	145
50	61	71	87	111	121	142	158
100	108	115	127	147	155	174	189

150	156	161	170	186	193	209	222
200	204	208	215	228	234	247	259
250	253	256	262	272	277	288	298
300	302	305	309	317	321	330	339
350	352	354	357	364	367	375	382

BWR (9 x 9)

Nitrogen

$T_w(^{\circ}\text{C})/Q(\text{W})$	100	200	400	800	1000	1500	2000
25	34	42	57	80	89	110	127
50	58	65	78	99	108	127	143
100	106	111	121	138	146	162	177
150	154	158	166	180	186	200	213
200	203	206	213	224	229	241	252
250	253	255	260	269	273	283	293
300	302	304	308	315	319	327	335
350	352	353	356	363	366	373	380

BWR (9 x 9)

Argon

$T_w(^{\circ}\text{C})/Q(\text{W})$	100	200	400	800	1000	1500	2000
25	35	44	59	84	94	115	132
50	59	66	80	102	111	131	147
100	106	112	123	140	148	165	180
150	155	159	167	181	188	202	215
200	203	207	213	225	230	242	253
250	253	255	260	269	274	284	293
300	302	304	308	316	319	328	336
350	352	353	357	363	366	373	380

CFD Model (FLUENT): Figure 5(a) shows a temperature map for a 21 PWR (15 x 15) spent fuel assemblies in an evacuated canister with natural convection and radiation on the outer surface. The calculated PCTs and the canister surface temperatures are shown in Fig. 5(b) as a function of the

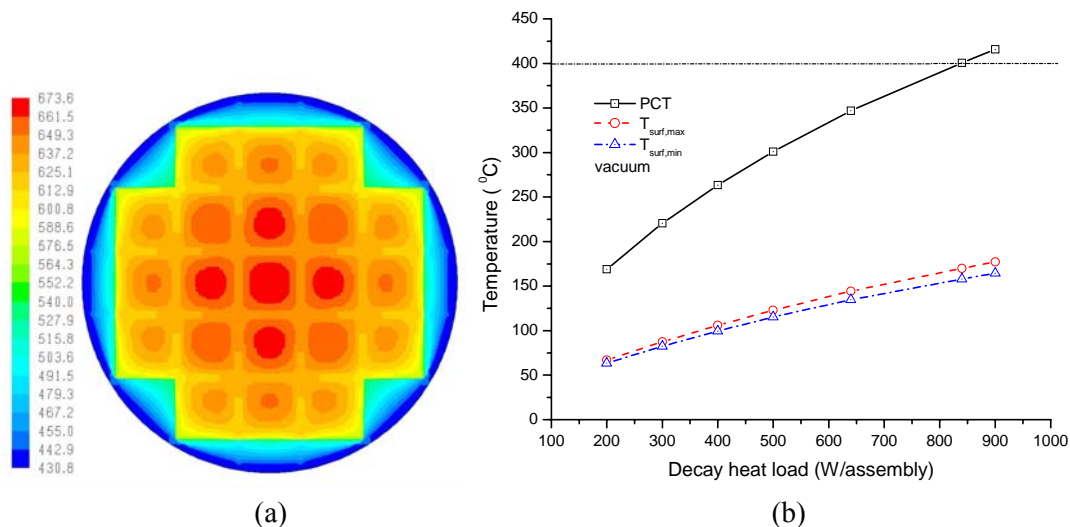


Fig. 5 Contour of temperature (in K) in a 21 PWR (15 x 15) spent fuel assemblies in an evacuated canister with assembly $Q = 840 \text{ W}$, (a); and calculated PCT and canister surface temperatures as a function of the assembly decay heat load, (b).

assembly decay heat load. The results showed that when the assembly decay heat load is 840 W, the calculated PCT can reach 400°C in an evacuated canister containing 21 PWR (15 x 15) spent fuel assemblies.

The CFD model is unique in its ability to quantitatively examine the influence of convection on heat transfer. The natural convection in a BWR (7 x 7) spent fuel assembly was numerically studied by comparing two simulations operating under nearly identical conditions, i.e., one takes into account conduction and radiation, while the other considers convection as well. Figure 6 shows the temperature contours of the two cases for a N₂-filled spent fuel assembly. The PCT in Fig. 6(b) with natural convection is slightly lower than the PCT in Fig. 6(a) without natural convection; however, the most dramatic effect of natural convection is revealed by the non-symmetrical temperature contour in Fig. 6(b), which is absent in Fig. 6(a).

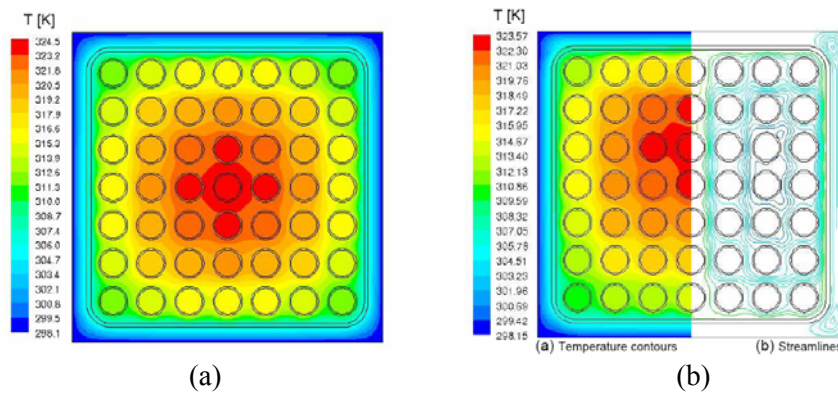


Fig. 6 Temperature contours (in K) for simulations of a BWR (7 x 7) spent fuel assembly with a heat load of 100 W, nitrogen backfill, and $T_w = 25^\circ\text{C}$: (a) radiation/conduction, and (b) radiation, natural convection, and conduction in solid components.

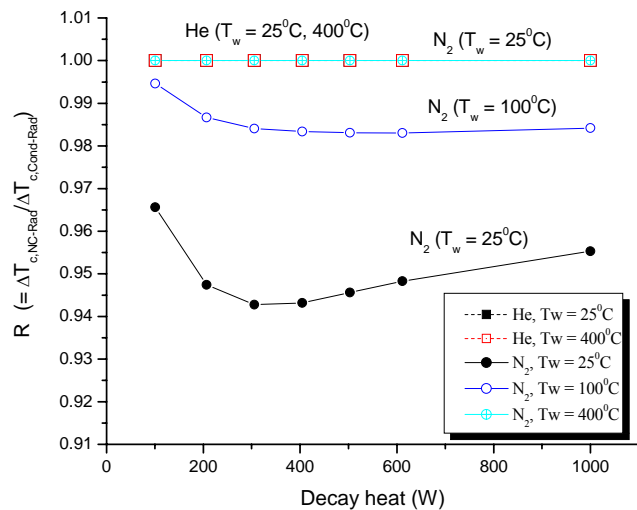


Fig. 7 Calculated ratio (R) of clad-to-wall temperature differences for radiation/natural convection ($\Delta T_{c, \text{NC-Rad}}$) and conduction/radiation ($\Delta T_{c, \text{Cond-Rad}}$)

Figure 7 summarizes the CFD simulation results for N₂- and helium-filled cases. The simulation results may be summarized as follows: (1) At $T_w = 400^\circ\text{C}$, the contribution of natural convection can be neglected because radiation heat transfer dominates due to its nonlinear temperature dependence, (i.e. $\approx T^4$). (2) For a high conductivity gas such as helium (He), the contribution of natural convection is limited at either elevated or low temperatures, as indicated by the overlapping curves of helium ($T_w = 25^\circ\text{C}$, 400°C) in Fig. 7.

The thermal conductivity of He is ≈ 10 times larger than that of nitrogen. Good thermal conduction reduces the temperature gradient across the entire fuel assembly, thereby effectively suppressing natural convection that depends non-linearly on the temperature gradient. For the N₂-filled case,

natural convection also lowers the PCTs particularly for low T_w (25°C) and low assembly decay heat load (≤ 300 W), as shown in the bottom curve of Fig. 7. The curve has an inflection point for N_2 ($T_w = 25^\circ\text{C}$); the inflection point is less obvious for the curve labeled N_2 ($T_w = 100^\circ\text{C}$).

Clarifying the role of natural convection is important because it gives insight on the relative significance of the three heat transfer processes, i.e., conduction, radiation, and convection. One needs to be careful when using an ETC-based model, for instance, in the calculation of PCTs for a poorly-conducting (gas) system at low temperature (T_w) and low assembly decay heat load, where natural convection could play a important role.

Comparison of calculated PCTs

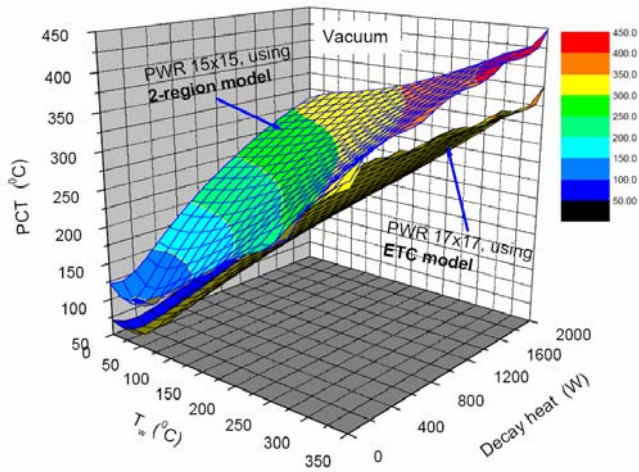


Fig. 8 The PCTs calculated by two-region model and ETC correlations.

Figure 8 compares the PCTs calculated for the PWR spent fuel assemblies in the vacuum environment by the ETC and two-region model. The difference is substantial in that the ETC model predicts a considerably lower PCT than that calculated based on the lumped k_{eff}/h_{edge} two-region model. For example, the PCT for a PWR (17 x 17) spent fuel assembly at decay heat $Q = 2,000$ W and $T_w = 150^\circ\text{C}$ is 209°C based on the ETC model, versus 351°C calculated for a PWR (15 x 15) assembly with the same Q and T_w , in vacuum.

Gomez and Greiner⁵ also compared the PCTs calculated by the ETC model and CFD simulation using the FLUENT CFD package. They performed 2-D numerical simulation of heat transfer in a BWR (7 x 7) spent fuel

assembly under a helium or nitrogen environment, for a range of decay heat loads (100 to 600 W) and wall temperatures (25 and 400°C). Again, the ΔT s obtained in the CFD simulation for the He environment at $T_w = 25^\circ\text{C}$ and 400°C are 14% and 40% higher, respectively, than those obtained by the ETC model of Bahney and Lotz.² For the nitrogen environment, the differences become even larger, up to 30% and 70%, respectively.

Figure 9 shows the PCTs calculated for a BWR (7 x 7) spent fuel assembly using FLUENT and the two-region model for a BWR (8 x 8) assembly. The limited CFD results, shown as colored dots in Fig. 9, are surprisingly close to the PCTs obtained by the two-region model. This indicates that the two-region model is somewhat

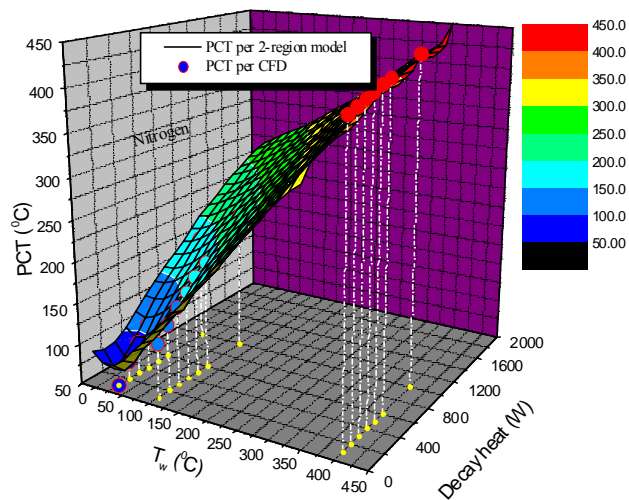


Fig. 9 The PCTs calculated by the two-region model for a BWR (8 x 8) fuel assembly. The limited CFD results for a (7 x 7) assembly are plotted as colored dots.

conservative than the CFD model in calculating the PCT, since the average pin power in a BWR (8 x 8) assembly should lower than that in a BWR (7 x 7) assembly, for a given assembly power Q.

SUMMARY

A study has been conducted to identify suitable models that may be used to estimate the PCT of spent fuel assemblies in a storage or transportation cask. Three models were examined: A two-region model, an effective thermal conductivity (ETC) model, and a CFD model based on the FLUENT code. These models were used to calculate the PCTs for both PWR and BWR spent fuel assemblies under helium, nitrogen, and vacuum environments with varying decay heat loads and temperature boundary conditions. Regimes of assembly power and boundary temperature were mapped for each environment under which the calculated PCT would exceed a limiting temperature, e.g., 350°C.

The results clearly show that the vacuum environment is more challenging than nitrogen (taken as air) in that the PCT limit is exceeded at a lower boundary temperature for a given decay heat load of the assembly. The helium environment, on the other hand, produced PCTs exceeding 350°C in a few cases only, with high boundary temperature ($\geq 300^\circ\text{C}$) and high assembly power ($>1,500\text{ W}$). The most critical period that could affect cladding radial hydride formation is thus during vacuum drying; the current industry trend of higher power operation, higher burnup, and shorter cooling time increases the decay heat load in the spent fuel assembly, which would increase the PCT.

The ETC model calculated lower PCTs than those obtained by either the two-region model or the CFD model. The PCTs calculated by the two-region model and the CFD model are in reasonably good agreement for the limited cases studied in this paper. Uncertainties still remain in using these models. A coupled finite-element (for the heat transfer in solids) and CFD (for heat transfer in a fluid) model may be employed on a finer scale for future calculations of PCTs.

ACKNOWLEDGMENT

This work is supported by the U.S. Department of Energy, Environmental Management, Office of Safety Management and Operations (EM-60) under Contract DE-AC02-06CH11357. The U.S. Government retains for itself, and others acting on its behalf, a nonexclusive, royalty-free license with the rights to reproduce, to prepare derivative works, and to display publicly.

This work was prepared as an account of work sponsored by an agency of the United States Government. Neither the United States Government nor any agency thereof, nor UChicago Argonne, LLC, nor any of their employees or officers, makes any warranty, express or implied, or assumes any legal liability or responsibility for the accuracy, completeness, or usefulness of any information, apparatus, product, or process disclosed, or represents that its use would not infringe privately owned rights. Reference herein to any specific commercial product, process, or service by trade name, trademark, manufacturer, or otherwise, does not necessarily constitute or imply its endorsement, recommendation, or favoring by the United States Government or any agency thereof. The views and opinions of document authors expressed herein do not necessarily state or reflect those of the United States Government or any agency thereof, Argonne National Laboratory, or UChicago Argonne, LLC.

REFERENCES

1. R. D. Manteuffel and N. E. Todreas, *Effective Thermal Conductivity and Edge Conductance Model for a Spent Fuel Assembly*, Nucl. Technol., Vol. 105, p. 421, 1994.

2. R. H. Bahney and T. L. Lotz, *Spent Nuclear Fuel Effective Thermal Conductivity Report*, U.S. Department of Energy, BBA000000-01717-5705-00010 REV 00, July 11, 1996.
3. *Cladding Considerations for Transportation and Storage of Spent Fuel*, Nuclear Regulatory Commission Interim Staff Guidance (ISG)-11, Rev. 3, November 17, 2003.
4. R. S. Daum, S. Majumdar, Y. Liu, and M. C. Billone, *Radial-hydride Embrittlement of High-burnup Zircaloy-4 Fuel Cladding*, *Journal of Nuclear Sci. and Tech.*, Vol. 43, pp. 1054–1067, April 2006.
5. P. E. A. Gomez and M. Greiner, *Simulation of Heat Transfer within the Fuel Assembly/ backfill Gas Region of Transport Packages*, Proc. ASME PVP Conf., Denver, Colo., July 17-21, 2005.
6. *Multi-Purpose Canister (MPC) Implementation Program Conceptual Design Phase Report*, Office of Civilian Radioactive Waste Management (OCRWM), U.S. Department of Energy, A20000000-00811, 1993.
7. *Transport, Aging and Disposal Canister System Performance Specification*, Rev. 0, Office of Civilian Radioactive Waste Management (OCRWM), U.S. Department of Energy, DOE/ RW-0585, June 2007.